Environ. Sci. Technol. **2006**, *40,* 1884−1891

Interactions between Microbial Iron Reduction and Metal Geochemistry: Effect of Redox Cycling on Transition Metal Speciation in Iron Bearing Sediments

D. CRAIG COOPER,*,† FLYNN F. PICARDAL,‡ AND AARON J. COBY‡

Geosciences Research, Idaho National Laboratory, P. O. Box 1625, MS 2107, Idaho Falls, Idaho 83415-2107, and School of Public and Environmental Affairs, Indiana University, Bloomington, Indiana 47405

Microbial iron reduction is an important biogeochemical process that can affect metal geochemistry in sediments through direct and indirect mechanisms. With respect to Fe(III) (hydr)oxides bearing sorbed divalent metals, recent reports have indicated that (1) microbial reduction of goethite/ferrihydrite mixtures preferentially removes ferrihydrite, (2) this process can incorporate previously sorbed Zn(II) into an authigenic crystalline phase that is insoluble in 0.5 M HCl, (3) this new phase is probably goethite, and (4) the presence of nonreducible minerals can inhibit this transformation. This study demonstrates that a range of sorbed transition metals can be selectively sequestered into a 0.5 M HCl insoluble phase and that the process can be stimulated through sequential steps of microbial iron reduction and air oxidation. Microbial reduction experiments with divalent Cd, Co, Mn, Ni, Pb, and Zn indicate that all metals save Mn experienced some sequestration, with the degree of metal incorporation into the 0.5 M HCl insoluble phase correlating positively with crystalline ionic radius at coordination number = 6. Redox cycling experiments with Zn adsorbed to synthetic goethite/ferrihydrite or iron-bearing natural sediments indicate that redox cycling from iron reducing to iron oxidizing conditions sequesters more Zn within authigenic minerals than microbial iron reduction alone. In addition, the process is more effective in goethite/ferrihydrite mixtures than in iron-bearing natural sediments. Microbial reduction alone resulted in a ∼3× increase in 0.5 M HCl insoluble Zn and increased aqueous Zn (Zn-aq) in goethite/ferrihydrite, but did not significantly affect Zn speciation in natural sediments. Redox cycling enhanced the Zn sequestration by ∼12% in both goethite/ferrihydrite and natural sediments and reduced Zn-aq to levels equal to the uninoculated control in goethite/ferrihydrite and less than the uninoculated control in natural sediments. These data suggest that in situ redox cycling may serve as an effective method for mitigating divalent metal contamination in subsurface environments.

Introduction

Dissimilatory reduction of iron oxide minerals has been documented for a large number of microorganisms in a wide range of environments (*1*−*3*), is an important constituent of the global carbon and iron cycles (*2*, *4*−*7*), and has a profound effect on metal geochemistry in groundwater and sedimentary environments. Since iron (hydr)oxides are important sorbents of trace metals in many soils and sediments, microbially mediated changes of the (hydr)oxide can have an important impact on the mobility of contaminant metals. The impact of microbial iron reduction on sediment mineral composition and metal geochemistry has been extensively researched (*8*−*14*), with most studies examining the ability of dissimilatory metal reducing bacteria (DMRB) to directly and indirectly alter the oxidation state of redox-reactive, multivalent metals such as arsenic, chromium, and uranium. With respect to the effect of DMRB activity on the cycling of common transition metals, Zachara et al. (*15*) have demonstrated that microbial Fe(II) production can alter the sorption of Co(II) to goethite in the presence of EDTA. DMRB activity produces Fe(II) that competes with Co(II) for EDTA ligands, increasing the proportion of adsorbed Co(II) and reducing cobalt mobility. Microbial reduction of Ni(II)- and Co(II)-substituted goethite can release these metals into solution (*12*, *14*), and microbial iron reduction can also mobilize previously adsorbed arsenic (*16*). Kamon et al. (*17*) have indicated that Zn(II) mobility in a clay landfill liner increases under iron reducing conditions, with sulfide minerals controlling Zn(II) solubility under SO_4^{2-} reducing conditions. Using iron (hydr)oxides bearing sorbed Zn, Cooper et al. (*18*, *19*) have also reported that microbial iron reduction can lead to slightly elevated levels of aqueous Zn(II), while concomitantly increasing the amount of solid-associated Zn(II) that is insoluble in 0.5 M HCl. This change in Zn(II) speciation is directly proportional to the amount of ferrihydrite present, and likely results from Fe(II) reacting with ferrihydrite to nucleate goethite (*20*, *21*) and catalyze Zn(II) incorporation into authigenic goethite. Taken together, these studies indicate that (1) microbial iron reduction may tend to increase the aqueous concentration(s) of divalent metals in the absence of complexing agents; (2) that Fe(II) production impacts divalent metal sorption properties; and (3) that iron reduction in the presence of ferrihydrite can alter the speciation of adsorbed metals by incorporating them into a solid phase that is not soluble at low pH. This solid phase is likely authigenic goethite (*18*), but the reports are not conclusive in this regard.

The observed combination of increased metal release to solution as surface sites are destroyed and increased metal resistance to acid dissolution arising from microbial iron reduction is intriguing and, at first perhaps, counterintuitive. Increases in trace metal solubility could be explained partially by a decrease in (hydr)oxide surface area and sorption sites as a result of reductive dissolution of the sorbent, with biogenic Fe^{2+} competing with metals for sorption sites in sediments (*15*). Sequestration of previously adsorbed metals into 0.5 N HCl-insoluble phases occurs concomitantly with increases in aqueous solubility of these metals, and is thought to occur via incorporation of metals into the matrix of authigenic crystalline minerals that form as a result of dissolution−precipitation reactions between Fe(II) and fer-

* Corresponding author phone: 208-526-5395; fax: 208-526-0875; e-mail: Craig.Cooper@inl.gov.
† Idaho National Laboratory.
‡ Indiana University.

10.1021/es051778t CCC: $33.50

Published on Web 02/09/2006

rihydrite (*18*−*22*). This sequestration process can be mitigated by nonreducible adsorbing minerals, such as 1:1 clays, that provide alternate sites for metal sorption. This has been demonstrated through studies that report microbial iron reduction can shift previously adsorbed Zn(II) from surface complexes with iron oxide minerals to outer-sphere $ZnCl_2$ complexes that are likely associated with clay mineral surfaces (*18*).

The combination of these previous studies suggests that ferrihydrite is a key reactive mineral that can drive metal sequestration into stable iron oxides, as long as nonreducible minerals do not re-adsorb metals released from iron oxides as a result of microbial iron reduction. These conclusions with respect to Zn(II) raise two questions: (1) does this effect extend to other metals?, and (2) can it be stimulated through cycling between reducing and oxidizing conditions? This study seeks to answer these questions by performing two sets of experiments. First, we determine if microbial iron reduction, in the presence of ferrihydrite, can sequester a range of divalent metals into a 0.5 M HCl insoluble phase. Second, we determine if sequential reduction, air-oxidation, and reestablishment of anaerobic conditions can enhance the proportion of "strongly bound" zinc (insoluble in 0.5 M HCl) in both natural sediments and synthetic iron oxides. This study is a follow-up to the previously reported work of Cooper et al. (*18*), and we have adopted their methods and choice of primary metal (Zn). We have also utilized the same sediments used in their prior work, synthetic very high surface area (VHSA) goethite and natural iron−kaolinite−quartz sediment.

Materials and Methods

Sediment Characterization. The sediments used in these experiments have been previously described (*18*, *19*). Briefly, the synthetic, VHSA goethite is a fine-grained mixture of goethite (∼93%) and ferrihydrite (∼7%) with a high surface area (95 $m^2\ g^{-1}$) and all particles less than 150 μm in diameter. Sediment Fe−K−Q is a clayey sand with moderate surface area (38 $m^2\ g^{-1}$), a cation exchange capacity (CEC) of ∼12 ± 5 mmol charge 100 g^{-1}, and ∼5% citrate dithionite (DCB) extractable iron by mass. Most of the iron in sediment Fe−K−Q is found in the smaller grain size fractions, with ∼75% associated with hematite and the remainder associated with fine-grain phyllosilicates that are predominantly kaolinite with traces of illite. Chemical extraction data from these studies (*18*) suggested that some ferrihydrite may be present in sediment Fe−K−Q, but likely constitutes less than 1% of total sedimentary iron. The main geochemical differences between these two sediments arise from (1) surface area, (2) the presence of nonreducible clay minerals in sediment Fe−K−Q, and (3) the identity of the primary iron oxide mineral (ferriydrite/goethite versus hematite).

Microorganism and Culture Conditions. *Shewanella putrefaciens* is a Gram negative, motile rod with an obligate respiratory metabolism (*23*). The strain used in these experiments, *S. putrefaciens* 200, was originally isolated from a Canadian oil pipeline by Obuekwe (*24*). The culture was maintained on solid medium of nutrient agar containing 5 g L^{-1} yeast extract (Difco, Detroit, MI) as previously described (*25*). Liquid cultures were grown in a 2.5-L Bioflow 3000 Fermentor (New Brunswick Scientific Company, Edison, NJ) in a medium that consisted (per liter) of 2.0 g Na_2SO_4, 0.5 g K_2HPO_4, 1.0 g NH_4Cl, 0.198 g $CaCl_2{\cdot}2H_2O$, 0.1 g $MgSO_4{\cdot}7H_2O$, 19.35 mg $FeCl_3{\cdot}6H_2O$, 0.5 g yeast extract, and 3 mL of 60% (w/v) sodium lactate. Following an initial period of aerobic growth, anaerobic reductase activity was induced by reducing the air-flow to approximately 100 mL min^{-1} and maintaining the cells under suboxic ($[O_2]_{(aq)}$ < 2.5 μmol L^{-1}) conditions for a period of 12 h. *S. putrefaciens* cells were harvested by centrifugation and re-suspended in a cell concentrate to a target optical density (A_{600} = ∼1.2) in artificial groundwater (AGW) medium. Small aliquots of this cell concentrate were subsequently used to inoculate the experimental slurries.

Iron Reduction Experiments with Zn^{2+} and Various Solid-Phase Fe(III) Substrates. The anoxic artificial groundwater medium (AGW) and VHSA goethite (∼95 m^2/g) used in these experiments have been described previously (*18*, *19*). The AGW medium used in these experiments also contained 10 mmol L^{-1} HEPES buffer and 10 mmol L^{-1} lactate as a carbon source. An anoxic Zn^{2+} stock solution was prepared by dissolving zinc chloride salt in Milli-Q water and adjusting it to pH 6.0 with 10.0 M NaOH. This stock solution was sterilized by autoclaving and an aliquot was subsequently added to the AGW media so that the concentration of total exogenous Zn^{2+} was 200 μmol L^{-1}. The natural iron−kaolinite−quartz sediment (Fe−K−Q) was not washed or otherwise modified prior to experimentation. To prepare the experimental slurry, enough sediment to account for 1 mmol of citrate dithionite extractable iron (c.a. 0.09 g VHSA goethite, 1.3 g Fe−K−Q per tube) was added to a set of acid-washed glass anaerobic culture (Balch) tubes (Bellco, 25 mL nominal volume). The tubes were autoclaved and subsequently cooled in an anaerobic chamber (Coy Laboratory Products) containing 95% N_2 and 5% H_2. Under anaerobic conditions, 20 mL of lactate, HEPES, and Zn^{2+} amended sterile AGW medium was added to the tubes. The tubes were then crimp sealed with acid-washed, butyl rubber stoppers and allowed to equilibrate on a shaker table (horizontal orientation) for a period of 7 days. Previous experiments have indicated that pH and aqueous metal concentrations typically reach an approximate steady-state condition within one week, with subsequent changes being slow and of small magnitude. The bottle headspace in all cases was 95%:5% N_2/H_2, and the sediment in the tubes was manually re-suspended once per day.

Prior to inoculation with *S. putrefaciens*, an initial set of samples (t_0) was taken to provide baseline characterization. Because of the difficulty in obtaining repeatable aliquots of coarse-grained sediments from suspended slurries, 4 sets of 5 Balch tubes (3 inoculated and 2 uninoculated) were "sacrificed" at each sampling interval. Each set of 5 tubes contained one sediment type (VHSA goethite, sediment Fe−K−Q). Reported values reflect the average and standard deviation of analyses conducted on tubes sampled at the same time. For the purpose of comparison, all tubes are assumed to be equivalent aliquots of one large set. Fe(III) reduction experiments were initiated by inoculating slurries with 0.5 mL of *S. putrefaciens* suspension under anaerobic conditions. After dilution, this resulted in an estimated initial culture optical density (A_{600}) of 0.020, which corresponded to approximately 2×10^6 cells mL^{-1}. At each periodic sampling point, a set of Balch tubes was removed from the shaker table, manually inverted to resuspend any settled solids, and then centrifuged (30 min, 4000*g*) to separate liquid from solid. The centrifuged tubes were then transferred to the anaerobic chamber, opened, and sampled for pH, aqueous Fe(II), and aqueous Zn^{2+}. Excess supernatant was decanted, the sediments were re-suspended in 20 mL of 0.5 M HCl, the tubes were re-sealed inside the anaerobic chamber, and then the tubes were transferred to a rotary mixer where they were digested for 2 h at room temperature. After this digestion, the tubes were centrifuged (30 min, 4000*g*) and the supernatant was sampled for "bound" Fe(II) and Zn^{2+} (bound = solid fraction that is soluble in 0.5 M HCl). The remaining supernatant was decanted and the solid pellet was re-suspended in 6.0 M HCl and digested for a period of 72 h. After this final digestion, the tubes were centrifuged (30 min, 4000*g*) and the supernatant was sampled for "strongly bound" Zn^{2+} (strongly bound = solid fraction that is not soluble in 0.5 M HCl).

With noted exceptions, experiments involving sequential microbial reduction, Fe(II) oxidation, and microbial rereduction were conducted according to the procedure described above. For these experiments, two sets of 5 tubes (3 inoculated, 2 uninoculated) were sampled at each time point prior to oxidation and two sets of 10 tubes (3 inoculated + 2 uninoculated exposed to oxidation and rereduction, 3 inoculated + 2 uninoculated *not* exposed to oxidation and rereduction) were sampled at each time point thereafter. Oxidation was accomplished by thoroughly flushing the headspace of the "oxidized" tubes with sterile air twice within a period of 12 h. Anaerobic conditions were reestablished by thoroughly flushing the headspace of the "oxidized" tubes with sterile, ultrahigh purity N_2 at the end of the 12 h oxidation period (10 min per tube, flow rate of 50 mL/min). Sets of samples were taken at several time points prior to oxidation, immediately prior to oxidation, immediately after oxidation, and at two time points after the air removal.

Iron Reduction Experiments with VHSA Goethite and Cd^{2+}, Co^{2+}, Mn^{2+}, Ni^{2+}, Pb^{2+}, or Zn^{2+}. With noted exceptions, the artificial groundwater medium (AGW) and synthetic VHSA goethite was synthesized according to the procedures described above. Sterile, anaerobic stock solutions of Cd^{2+}, Co^{2+}, Mn^{2+}, Ni^{2+}, Pb^{2+}, or Zn^{2+} were prepared from the respective chloride salts dissolved in Milli-Q water and adjusted to pH 6.0 with 10.0 M NaOH (pH 5.5 for Pb^{2+}). As required, aliquots of these stock solutions were added to the AGW media so that the concentration of total exogenous metal was 100 μmol L^{-1} (25 μmol L^{-1} for Pb^{2+}). Individual sets of AGW medium were synthesized for each metal treatment. For these experiments, the use of fine-grained VHSA goethite as an Fe(III) substrate allowed repeatable sampling of aqueous slurries and sacrifice of replicate tubes was not necessary. Although the technique used in these experiments has been previously described (*18*, *19*), a brief summary is presented here. The experimental slurries were prepared by adding 0.5 g of sieved goethite to acid-washed, glass serum bottles (nominal 160-mL volume), autoclaving, and cooling as previously described for Balch tubes. While maintaining anaerobic conditions, 125 mL of sterile, metal-amended AGW medium was added to the bottles and the bottles were crimp-sealed with an acid-washed butyl rubber stopper. The bottles were equilibrated on a shaker table for a period of 7 days, an initial sample (t_0) was taken prior to inoculation, and the t_0 samples were treated as previously described. Experiments were initiated by inoculating slurries with 2.0 mL of a *S. putrefaciens* suspension concentrated enough to produce 2×10^6 cells mL^{-1} in the sediment slurry. Except for the use of small aliquot volumes and ~2.0 mL Eppendorf centrifuge tubes for the separation steps, sediment digestions and operations were carried out as previously described. Also, total metal was measured in a separate aliquot and "strongly bound" metal was defined as the difference between total metal added and the sum of the aqueous and "bound" fractions.

Analyses and Sediment Characterization. Aqueous Fe(II) and bound Fe(II) were analyzed immediately after sampling via a modified version of the colorimetric ferrozine technique (*26*, *27*). Acidified aqueous, bound, and strongly bound Zn were stored in acid-washed polyethylene bottles until they could be analyzed via flame atomic absorption spectrophotometry (AAS). Solution pH was measured inside the anaerobic chamber with a Cole Parmer glass electrode calibrated with pH 4 and pH 7 standard NBS buffers. The concentration of Cd^{2+}, Co^{2+}, Mn^{2+}, Ni^{2+}, Pb^{2+}, and Zn^{2+} in acidified extracts was determined by flame AAS using a Perkin-Elmer 4100 flame atomic absorption spectrophotometer. For colorimetric analysis of ferrozine-treated Fe(II) samples, the absorbance at 562 nm was measured on a Schimadzu UV-2101PC UV/VIS spectrophotometer. Metal standards for AAS analysis were prepared by diluting aliquots of certified commercial standards in 0.5 M HCl, and Fe(II) standards were diluted from a concentrated stock solution of ferrous sulfate in 0.5 M HCl. Unless otherwise noted, all solutions were prepared in Milli-Q water (R = 18 MΩ). All experiments, extractions, and analyses were performed in acid-washed glassware and plasticware, and procedural blanks consisting of Milli-Q water were sampled regularly to monitor for potential metal contamination.

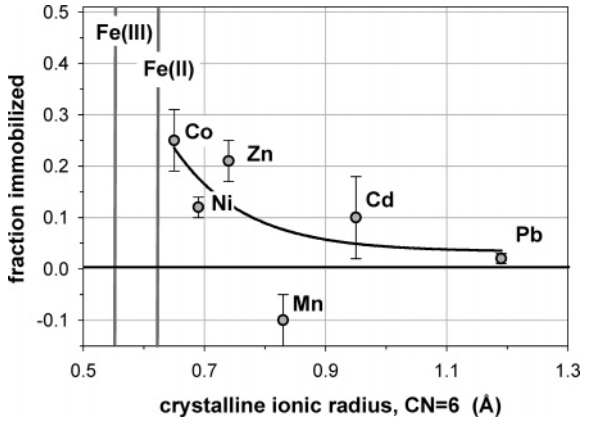

FIGURE 1. Plot of fraction of metal immobilized versus the metal's ionic radius in octahedral coordination (CN = 6) for experiments conducted with VHSA goethite. Vertical lines represent ionic radius of Fe(II) and Fe(III), and error bars represent the standard deviation between triplicate samples. The fraction of metal immobilized = ([strongly bound metal]$_{inoculated}$ − [strongly bond metal]$_{uninoculated}$) /[total metal]. [Strongly bound metal] = [total metal] − [0.5 N extractable metal] − [aqueous metal]. Fraction immobilized is calculated from the difference between the inoculated sample and uninoculated control over the final three sampling periods.

Results

Effect of Microbial Iron Reduction on Previously Sorbed, Divalent Metals. Data describing the effect(s) of microbial iron reduction of VHSA goethite on the speciation of previously adsorbed Cd(II), Co(II), Mn(II), Ni(II), Pb(II), and Zn(II) are provided in Figure 1. These data are presented as the fraction of total metal that is not soluble in 0.5 M HCl (fraction immobilized) at the final time-point (500 h) versus the ionic radius of the metal in an oxide crystal with coordination number equal to six. For all metals, the degree of immobilization at the initial time point (168 h) was within the error bars given for the final time point (500 h). Greater than 75% of total Fe(II) was produced within the first 168 h, and Fe(II) was slowly produced throughout the experiment. This time-trend is consistent across all metal slurries, and agrees with previous reports for Fe(II) production in batch studies of iron reduction with a solid substrate. All inoculated slurries generated 6−7 mM Fe(II) over the course of the experiment, except Cd (~1 mM) and Pb (~4.5 mM). For all slurries, save Pb, pH was 7.0 ± 0.1 for both inoculated and uninoculated systems. For Pb, pH was ~6.5 ± 0.1 for both inoculated and uninoculated systems. All metal speciation data has been normalized to the uninoculated control sample. For Zn(II), the fraction of Zn(II) immobilized into a 0.5 M HCl insoluble phase is similar to what has been previously reported (*18*, *19*). The solid-phase speciation data (Figure 1) indicate that the degree of divalent metal immobilization generally correlates with the ionic radius of that metal in a crystal where the basic structural unit is an octahedron (CN = 6). With the exception of Mn(II), divalent metals with an ionic radius under octahedral coordination (CN = 6) more similar to that of iron experience a greater degree of reductive immobilization. Similar comparisons with charge function

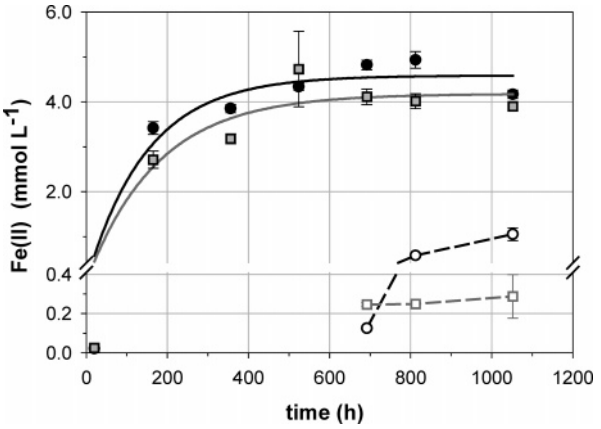

FIGURE 2. Trends in the sum of aqueous and 0.5 M HCl soluble Fe(II) as a function of time for VHSA goethite (circles) and Fe−K−Q (squares). Closed symbols represent microbially reduced systems that were never air-oxidized. Open symbols represent similar systems that were oxidized (∼700 h) and then purged with UHP N_2 to re-establish anoxic conditions as described in the text. The data point at ∼700 h was determined immediately after oxidation and prior to purging with N_2. Error bars represent the standard deviation between triplicate samples, and trend lines are for illustrative purposes only. Note the break in the *y*-axis. Fe(II) production was not observed in uninoculated controls.

and first hydrolysis constant do not yield a similarly consistent trend (data not shown).

Effect of Redox Cycling on Fe(II) Concentrations in VHSA Goethite and Fe−K−Q. Data describing the effect(s) of sequential iron reduction, air-oxidation, and reestablishment of anaerobic conditions on Fe(II) speciation in these two sediments are provided in Figure 2. Data for pH and aqueous Fe(II) are similar to what has been previously reported (*18*, *19*), and data are shown only for the sum of aqueous and 0.5 M HCl-extractable Fe(II). For reference, pH ranges from 6.8 to 7.2 in reduced samples, and aqueous Fe(II) contributes 25−50% of total Fe(II). In oxidized samples, pH ranges from 6.4 to 6.8 with no discernible time trend. The iron reduction portion of these data indicate that ∼10% of total dithionite-reducible iron is reduced in these experiments. These results are in good agreement with previous studies conducted under analogous conditions (*18*, *19*, *28*), indicating that the biogeochemical conditions within these experiments are comparable to those in previous reports. Microbial reduction of VHSA goethite produced Fe(II) at a fast initial rate, which then decreased and Fe(II) concentrations asymptotically approached a final concentration of ∼4800 μmol Fe(II)-tot L^{-1} (sum of aqueous and 0.5 M HCl-extractable). Microbial Fe−K−Q reduction produced similar trends, with Fe−K−Q Fe(II) concentrations asymptotically approaching final concentrations of ∼4000 μmol Fe(II)-tot L^{-1}. Fe(II) production was not observed in the uninoculated controls (data not shown).

Upon air-oxidation, total 0.5 M HCl soluble Fe(II) in all oxidized slurries decreased to less than 0.25 mM in both slurries while aqueous Fe(II) decreased to below detection limits (aqueous Fe(II) data not shown). Fe(II)-tot in VHSA goethite decreased to less than 0.1 mM while Fe(II)-tot in sediment Fe−K−Q only decreased to ∼0.25 mM, indicating that surface-associated Fe(II) in sediment Fe−K−Q may be more resistant to air-oxidation than is Fe(II) in synthetic VHSA goethite. After air-oxidation, the headspace was flushed with N_2 to eliminate headspace O_2 and speed reestablishment of iron-reducing conditions. During this putative rereduction step, both aqueous and 0.5 M HCl soluble Fe(II) slowly increased in VHSA goethite but did not change in sediment Fe−K−Q during ∼2 weeks of subsequent incubation under anaerobic conditions.

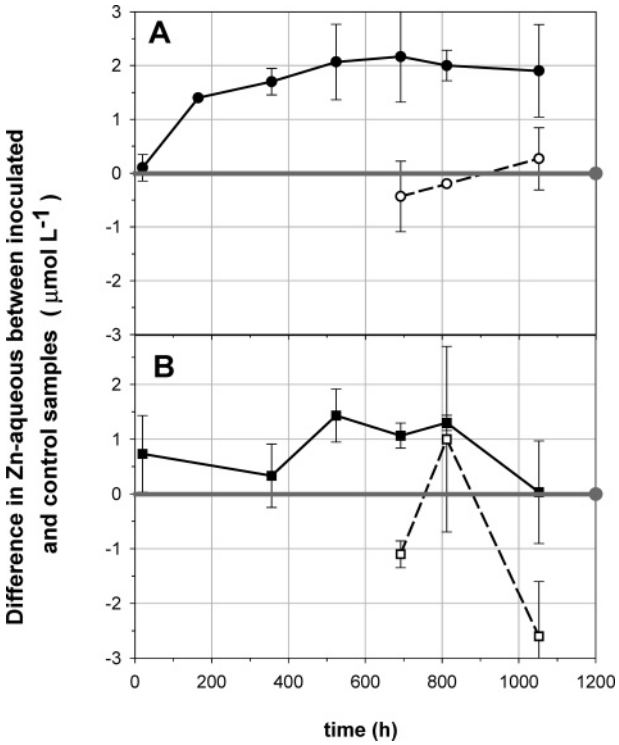

FIGURE 3. Time trends denoting the effect of microbial iron reduction on aqueous zinc for VHSA goethite (A) and Fe−K−Q (B). Closed symbols represent systems that were never air-oxidized. Open symbols represent systems that were oxidized (∼700 h) and then purged with UHP N_2 to reestablish iron-reducing conditions as described in the text. The data point at ∼700 h was determined immediately after oxidation and prior to purging with N_2. Error bars represent the standard deviation between triplicate samples. Negative values denote samples where the inoculated system had *less* Zn-aq than the uninoculated control.

Effect of Redox Cycling on Zn(II) Speciation in VHSA-G Goethite and Fe−K−Q. The effect of redox cycling, as demonstrated by changes in Fe(II), on Zn(II) concentrations is different for aqueous and 0.5 M HCl soluble Zn in the two different sediment systems. These data are presented in terms of the difference between an inoculated sample and uninoculated control, rather than the measured concentrations in inoculated and control experiments. This was done to simplify data presentation while accounting for slow abiotic changes in Zn speciation that can occur in long-term experiments as a result of sorption processes and diffusion into micropores. Within experimental precision, the sum of individual species matched the total Zn added, indicating that all Zn was recovered (data not shown).

For aqueous Zn, data describing the effect(s) of sequential iron reduction, air-oxidation, and reestablishment of anaerobic conditions in these two sediments are provided in Figure 3. In VHSA goethite, Zn-aq in uninoculated controls decreased from 1.4 ± 0.2 at t_0 to an average 0.3 ± 0.2 μmol L^{-1} over the last three time points (4−6 weeks). In the inoculated, unoxidized VHSA goethite samples, Zn-aq increased from 1.4 ± 0.2 at t_0 to 2.3 ± 0.2 μmol L^{-1} over the same time period. This yields a net increase of ∼2 μmol L^{-1} Zn-aq as a result of microbial iron reduction in VHSA goethite. In sediment Fe−K−Q, Zn-aq in uninoculated controls decreased from 8.6 ± 0.8 at t_0 to 6.3 ± 0.4 μmol L^{-1} over the last three time points (4−6 weeks). In the inoculated, unoxidized Fe−K−Q samples, Zn-aq decreased from 8.6 ± 0.8 at t_0 to 7.3 ± 0.7 μmol L^{-1} over the same time period. This yields a net increase

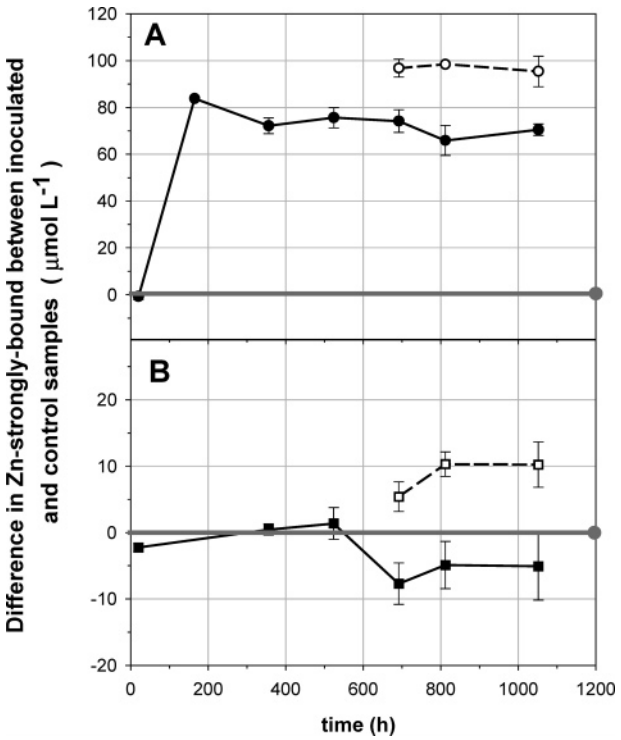

FIGURE 4. Time trends showing the effects of microbial iron reduction on strongly bound Zn (0.5 M HCl insoluble) for VHSA goethite (A) and Fe−K−Q (B). Closed symbols represent systems that were never air-oxidized. Open symbols represent systems that were first oxidized (~700 h) and then purged with UHP N_2 as described in the text. The data point at ~700 h was determined immediately after oxidation and prior to purging with N_2. Error bars represent the standard deviation between triplicate samples. Negative values denote samples where the inoculated system had *less* Zn-str-bnd than the uninoculated control. Higher values represent a greater degree of Zn immobilization.

of ~1 μmol L^{-1} Zn-aq for 3 of 4 sampling points as a result of microbial iron reduction in sediment Fe−K−Q, a change that is approximately equal to the standard deviation between three replicate samples. Upon air-oxidation of reduced samples, Zn(II)-aq decreased to levels lower than the uninoculated control in both VHSA goethite and sediment Fe−K−Q. The effect is most easily observed in VHSA goethite, but may have resulted in a greater net decrease of Zn(II)-aq in Fe−K−Q, where Zn(II)-aq concentrations are generally much lower in the reduced/air-oxidized system than in the uninoculated control (note the large error bars at the t = ~800 h time point for Fe−K−Q). Reestablishment of anaerobic conditions in these slurries did not significantly alter Zn(II)-aq concentrations during ~2 weeks of subsequent incubation under anaerobic conditions.

Data describing the effect(s) of sequential iron reduction, air-oxidation, and reestablishment of anaerobic conditions on strongly bound Zn in these two sediments are provided in Figure 4. Note that an increase in strongly bound zinc reflects a decrease in Zn(II) that is either aqueous or extractable in 0.5 M HCl. Previous studies have indicated that this strongly bound Zn(II) fraction is likely coprecipitated with authigenic goethite that forms as a result of chemical reactions between Fe(II) and ferrihydrite present in the original samples (*18*). In VHSA goethite, strongly bound Zn in uninoculated control samples increased from 72.1 ± 1.3 at t_0 to an average 107.8 ± 6.5 μmol L^{-1} over the last three time points (4−6 weeks). In the inoculated, unoxidized VHSA goethite samples, strongly bound Zn increased from 72.1 ± 1.3 at t_0 to 178.0 ± 4.0 μmol L^{-1} over the same time period. This yields a net increase of ~70.2 μmol L^{-1} strongly bound Zn as a result of microbial iron reduction in VHSA goethite. In sediment Fe−K−Q, strongly bound Zn in uninoculated controls increased from 108.1 ± 1.3 at t_0 to 113.8 ± 14.4 μmol L^{-1} over the last three time points (4−6 weeks). In the inoculated, unoxidized Fe−K−Q samples, strongly bound increased from 108.1 ± 1.3 at t_0 to 114.6 ± 3.5 μmol L^{-1} over the same time period. This yields no significant net change in strongly bound Zn as a result of microbial iron reduction in sediment Fe−K−Q. Upon air-oxidation of reduced VHSA goethite samples, strongly bound Zn further increased to an average of 199.6 ± 6.4 μmol L^{-1} over the last three time points. In reduced Fe−K−Q samples, air oxidation increased strongly bound Zn to an average of 127.6 ± 4.2 μmol L^{-1} over the last three time points. This oxidation operation enhanced Zn sequestration into a 0.5 M HCl insoluble phase (likely goethite) by ~12% in both Fe−K−Q and VHSA goethite. Although subsequent reestablishment of anaerobic conditions stimulated a minor amount of iron reduction in VHSA goethite (Figure 2), further changes in Zn speciation after this reestablishment of anaerobic conditions cannot be resolved in either sediment (Figure 4).

Discussion

Previous studies have reported that microbial reduction of ferrihydrite-bearing sediments can result in immobilization of previously adsorbed Zn(II) into an 0.5 M HCl insoluble phase that is likely authigenic goethite (*18*). These experiments build upon this earlier work, and demonstrate that this process (1) selectively immobilizes metals according to atomic radius in an octahedral crystal, and (2) can be enhanced by redox cycling. These experiments do not directly investigate the role of ferrihydrite, as this issue was addressed in previously reported studies conducted concomitantly with these experiments (*18*). However, the role of ferrihydrite in mediating changes in sediment iron and metal speciation in response to redox shifts must be considered when interpreting the results reported herein.

Figure 5 presents a summary of proposed reaction mechanisms that are thought to affect divalent metal speciation in ferrihydrite-bearing systems. In Step 1, a mixture of iron-oxide minerals and ferrihydrite with previously adsorbed divalent metals (Me) is exposed to a dissimilatory iron-reducing microorganism. Microbially generated Fe(II) can enter the aqueous phase, adsorb to surfaces, or displace previously adsorbed metals (Step 2). Reactions between ferrihydrite and Fe(II) are known to induce goethite nucleation (*20*, *21*), and can incorporate previously adsorbed metals into the crystal matrix (*18*) (Step 3). Exposure to O_2 (Step 4), oxidizes microbially generated Fe(II) and nucleates new iron oxide minerals—generally mixtures of goethite and ferrihydrite (*29*). If operative in a natural system, this process can act to sequester metals into iron oxide minerals via either reduction of iron oxides in the presence of ferrihydrite, or through oxidation of Fe(II) generated via microbial iron reduction. Since Fe(II) oxidation can generate new ferrihydrite in addition to goethite (*29*), both the reduction and oxidation processes can be operative in any sediment−water system that is exposed to redox shifts.

Effect of Microbial Iron Reduction on Divalent Metal Speciation in VHSA-G Goethite. Iron reduction experiments conducted under both continuous-flow and batch conditions have indicated that Fe(II) addition to ferrihydrite can induce a ferrihydrite-to-goethite mineral transition that is partially dependent on the rate of Fe(II) production (*20*−*22*). Other reports have indicated that this transformation can act to incorporate previously adsorbed Zn(II) into an authigenic phase that is insoluble in 0.5 M HCl, likely goethite (*18*). The presence of nonreducible clay minerals can negate the effect of ferrihydrite transformations on Zn(II) sorption chemistry, and reduce the extent of immobilization. To maximize the

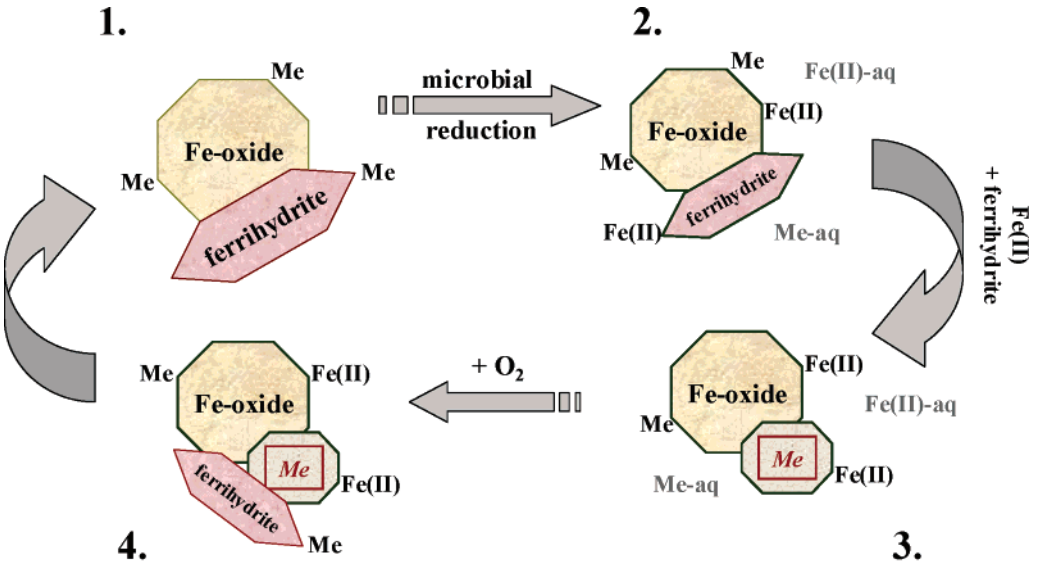

3

FIGURE 5. Schematic of proposed mechanism for the effects of redox cycling on divalent metal speciation in iron-bearing sediments. Numbers 1 to 4 refer to the proposed mechanistic steps as described in the text. Me = divalent metal. Octagons represent crystalline Fe (hydr)oxides (e.g., goethite, hematite).

extent of metal immobilization and more directly examine how the Fe(II)-ferrihydrite reactions affect the chemistry of different metals, the metal comparison experiments reported here were conducted in a ferrihydrite-bearing synthetic VHSA goethite in the absence of clay minerals.

The experiments reported here were performed with the same synthetic VHSA goethite used in these previous experiments (containing ~7% ferrihydrite), and were generally conducted concomitantly with these previously reported experiments (*18*). Microbial cultures, experimental conditions, and iron oxide materials were identical to this previous work; and the changes in iron and metal speciation during the reduction experiments with Zn were also analogous. Thus, we infer that the mineralogical changes observed in samples from parallel experiments also occur in the experiments reported here. The sole exception may be the Cd slurry, where we observed ~5× less Fe(II) production than in the other experiments. However, this slurry resulted in more metal immobilization than the Pb slurry that generated more Fe(II). No data are available on the relationship(s) between Fe(II) production rate and divalent metal immobilization that occurs as a result of the Fe(II)-driven ferrihydrite-to-goethite mineral transformation, and the relationship between Fe(II) production rate and the extent of metal immobilization cannot yet be resolved. However, results from this study suggests that there may not be a strong relationship between the processes that mediate metal immobilization in ferrihydrite bearing systems and the rate and extent of iron reduction.

These results indicate that microbial iron reduction in the presence of ferrihydrite selectively sequesters previously adsorbed divalent metals according to their atomic radius in an octahedral crystal. Cobalt, nickel, and zinc experienced the highest degree of immobilization, with cadmium and lead exhibiting much less immobilization. Lack et al. (*30*) observed a similar relationship in studies of metal sequestration during nitrate-dependent oxidation of Fe(II). U, Cd, and Co were removed from aqueous solution via coprecipitation into iron (hydr)oxides formed during Fe(II) oxidation, with the extent of removal from the aqueous phase likewise related to how similar the ionic radius of the metal was to that of iron. The basic structural unit of goethite is an octahedron (CN = 6) where a single Fe(III) atom is coordinated to six O(−II) or OH− ions (*29*). The direct correlation between the degree of metal immobilization and the divalent metal's ionic radius in octahedral coordination (CN = 6) is consistent with the hypothesis that Fe(II) production in the presence of ferrihydrite transforms that ferrihydrite into goethite via a dissolution/precipitation mechanism (*20*−*22*), allowing the incorporation of previously adsorbed metals into the crystal structure of the authigenic goethite (*18*). Divalent metals with an ionic radius more dissimilar to that of Fe(III) cause more deformities in the crystal structure, resulting in greater free energy barriers to nucleation and crystal growth. Divalent metals with an ionic radius more similar to that of Fe(III) have a lesser impact on crystal nucleation and growth, and are more likely to be incorporated within goethite. Manganese, which exhibited no immobilization, stands out as an exception to the observed trend between metal immobilization and ionic radius. This difference possibly arises from the tendency for Mn oxidation/reduction reactions to proceed much more quickly than those for iron and other transition metals (*31*). This unique behavior merits additional study, but does not detract from the general trend observed here.

Effect of Redox Cycling on Zn(II) Speciation in VHSA Goethite and Fe−K−Q. The combination of this study and previous work clearly indicate that microbial iron reduction in ferrihydrite-bearing systems can selectively incorporate a range of divalent metals into an authigenic mineral insoluble in 0.5 M HCl, likely goethite. The presence of nonreducible clay minerals can inhibit the extent of metal incorporation into this phase. The existence of this process, coupled to the clay mineral effect, raises the question of whether iron reduction, followed by Fe(II) reoxidation and oxidative iron oxide precipitation, can enhance metal sequestration into iron oxides. If operative, this process would enable a mechanism for redox cycling to drive natural attenuation of metal contamination. This study investigated this potential by following changes in Zn(II) speciation through a series of redox transformations in a goethite−ferrihydrite system (VHSA−G) and a hematite−quartz−clay system (sediment Fe−K−Q).

The results of this study suggest that sequential iron reduction, followed by Fe(II) oxidation, can act to immobilize divalent transition metals into an 0.5 M HCl insoluble phase

while also minimizing increases in aqueous metal concentration associated with iron reduction. The sequential reduction−oxidation process enhanced the extent of Zn immobilization in VHSA goethite and stimulated Zn immobilization in natural sediment where bio-reduction alone did not cause Zn immobilization. Reduction data are consistent with previous work (*18*, *19*), and the reoxidation data indicate that Fe(II) oxidation can immobilize additional sorbed metals into a phase not soluble in weak acid. The identity of the phase formed via reoxidation was not determined but it likely included a crystalline phase, e.g., goethite, with limited solubility in 0.5 N HCl. This observation on the effect of reoxidation on metal speciation is also consistent with previous work by others (*30*, *32*, *33*).

The sequential batch methodology used in this study only stimulated a minimal amount of microbial iron rereduction after the intermediate oxidation step. Although additional lactate was added during the rereduction stage, fresh cells were not, and the limited amount of rereduction may have reflected a decrease in cell viability or cell surface passivation via coatings of mixed Fe(II)−Fe(III) oxides formed during oxidation. Reactions between Fe(II) and oxidized nitrogen species (e.g., NO_3^-, NO_2^-) have been observed to form iron oxide coatings that can reduce the net rate of Fe(II) production, NO_3^- reduction, O_2 reduction, and fumarate reduction by *S. putrefaciens* (*34*, *35*). Thus, formation of iron oxide coatings by other means (e.g., chemical oxidation of Fe(II) by O_2) could also result in a reduction in cell activity. The response of a diverse microbial community that is adapted to unstable redox conditions in the environment as compared to the pure cultures used in our studies is unknown. This unresolved issue, in combination with the observation that the low extent of rereduction in these experiments had little effect on Zn speciation, highlights the need for future studies to investigate rates of iron redox cycling in natural systems, and how those rates affect metal speciation in diverse environments with varying amounts of ferrihydrite and clay minerals.

This study emphasizes the importance of iron redox cycling on driving changes in metal speciation in iron-bearing sediments, and highlights the relative importance of ferrihydrite and clay minerals in mediating these transformations. The new advance provided by this work is the observation that the overall cycle of reduction and oxidation can act in concert to reduce metal mobility to a greater extent than either oxidation or reduction alone. For divalent metals, the ability of this cycle to affect metal speciation is directly related to the metal's ionic radius in an octahedral crystal (CN = 6). This work suggests that bioremediation strategies involving sequential reduction and oxidation might have utility in reducing aqueous concentrations of divalent metals. In addition, biological processes regularly mediate the iron cycle in near-surface and subsurface systems (*3*, *36*, *37*), and thus cycling between Fe(III)-reducing and Fe(II)-oxidizing conditions may provide a mechanism for long-term, natural attenuation of divalent metal contamination. Further research is needed to establish the rates at which this process may occur under field conditions, and the effect of sediment mineral composition and fluid flow on this linkage between iron redox cycling and transition metal mobility.

Acknowledgments

We gratefully acknowledge the Department of Energy program in Natural and Accelerated Bioremediation (DOE grant DE-FG02-97ER62482) for funding this research, and the Idaho National Laboratory for supporting the preparation of this manuscript. We also thank Jason Rivera and the anonymous reviewers who helped improve this work.

Literature Cited

(1) Lloyd, J. R. Microbial reduction of metals and radionuclides. *FEMS Microbiol. Rev.* **2003**, *27*, 411−425.
(2) Lovley, D. R. Microbial Fe(III) reduction in subsurface environments. *FEMS Microbiol. Rev.* **1997**, *20*, 305−313.
(3) Lovley, D. R. In *Environmental Microbe-Metal Interactions*; Lovley, D. R., Ed.; ASM Press: Washington, DC, 2000; pp 3−30.
(4) Lovley, D. R. Dissimilatory Fe(III) and Mn(IV) reduction. *Microbiol Rev.* **1991**, *55*, 259−287.
(5) Konhauser, K. O. Diversity of bacterial iron mineralization. *Earth-Sci. Rev.* **1998**, *43*, 91−121.
(6) Lovley, D. R. Organic-matter mineralization with the reduction of ferric iron − a review. *Geomicrobiol. J.* **1987**, *5*, 375−399.
(7) Fredrickson, J. K.; Gorby, Y. A. Environmental processes mediated by iron-reducing bacteria. *Curr. Opin. Biotechnol.* **1996**, *7*, 287−294.
(8) Lovley, D. R. Dissimilatory metal reduction. *Annu. Rev. Microbiol.* **1993**, *47*, 263−290.
(9) Lloyd, J. R.; Chesnes, J.; Glasauer, S.; Bunker, D. J.; Livens, F. R.; Lovley, D. R. Reduction of actinides and fission products by Fe(III)-reducing bacteria. *Geomicrobiol. J.* **2002**, *19*, 103−120.
(10) Wielinga, B.; Bostick, B.; Hansel, C. M.; Rosenzweig, R. F.; Fendorf, S. Inhibition of bacterially promoted uranium reduction: Ferric (hydr)oxides as competitive electron acceptors. *Environ. Sci. Technol.* **2000**, *34*, 2190−2195.
(11) Fendorf, S.; Wielinga, B. W.; Hansel, C. M. Chromium transformations in natural environments: The role of biological and abiological processes in chromium(VI) reduction. *Int. Geol. Rev.* **2000**, *42*, 691−701.
(12) Fredrickson, J. K.; Zachara, J. M.; Kukkadapu, R. K.; Gorby, Y. A.; Smith, S. C.; Brown, C. F. Biotransformation of Ni-substituted hydrous ferric oxide by an Fe(III)-reducing bacterium. *Environ. Sci. Technol.* **2001**, *35*, 703−712.
(13) Fredrickson, J. K.; Zachara, J. M.; Kennedy, D. W.; Duff, M. C.; Gorby, Y. A.; Li, S.-m.; Krupka, K. M. Reduction of U(VI) in goethite(α-FeOOH) suspensions by a dissimilatory metal-reducing bacterium. *Geochim. Cosmochim. Acta* **2000**, *64*, 3085−3098.
(14) Zachara, J. M.; Fredrickson, J. K.; Smith, S. C.; Gassman, P. L. Solubilization of Fe(III) oxide-bound trace metals by a dissimilatory Fe(III) reducing bacterium. *Geochim. Cosmochim. Acta* **2001**, *65*, 75−93.
(15) Zachara, J. M.; Smith, S. C.; Fredrickson, J. K. The effect of biogenic Fe(II) on the stability and sorption of Co(II)EDTA(2-) to goethite and subsurface sediment. *Geochim. Cosmochim. Acta* **2000**, *64*, 1345−1362.
(16) Cummings, D. E.; Caccavo, F.; Fendorf, S.; Rosenzweig, R. F. Arsenic mobilization by the dissimilatory Fe(III)-reducing bacterium *Shewanella alga* BrY. *Environ. Sci. Technol.* **1999**, *33*, 723−729.
(17) Kamon, M.; Zhang, H. Y.; Katsumi, T. Redox effects on heavy metal attenuation in landfill clay liner. *Soils Found.* **2002**, *42*, 115−126.
(18) Cooper, C.; Neal, A.; Kukkadapu, R. K.; Brewe, D.; Coby, A. J.; Picardal, F. Effects of sediment iron mineral composition on microbially mediated changes in divalent metal speciation: importance of ferrihydrite. *Geochim. Cosmochim. Acta* **2005**, *69*, 1739−1754.
(19) Cooper, D. C.; Picardal, F.; Rivera, J.; Talbot, C. Zinc immobilization and magnetite formation via ferric oxide reduction by *Shewanella putrefaciens* 200. *Environ. Sci. Technol.* **2000**, *34*, 100−106.
(20) Hansel, C. M.; Benner, S. G.; Neiss, J.; Dohnalkova, A.; Kukkadapu, R. K.; Fendorf, S. Secondary mineralization pathways induced by dissimilatory iron reduction of ferrihydrite under advective flow. *Geochim. Cosmochim. Acta* **2003**, *67*, 2977−2992.
(21) Benner, S.; Hansel, C.; Wielinga, B.; Barber, T.; Fendorf, S. Reductive dissolution and biomineralization of iron hydroxide under dynamic flow conditions. *Environ. Sci. Technol.* **2002**, *36*, 1705−1711.
(22) Zachara, J. M.; Kukkadapu, R. K.; Fredrickson, J. K.; Gorby, Y. A.; Smith, S. C. Biomineralization of poorly crystalline Fe(III) oxides by dissimilatory metal reducing bacteria (DMRB). *Geomicrobiol. J.* **2002**, *19*, 179−207.
(23) Semple, K. M.; Westlake, D. W. S. Characterization of iron-reducing *Alteromonas putrefaciens* strains from oil field fluids. *Can. J. Microbiol.* **1987**, *33*, 366−371.
(24) Obuekwe, C. O. Microbial corrosion of a crude oil pipeline, Ph. D. Dissertation, Biology, Edmonton, Alberta, 1980.
(25) Picardal, F. W.; Arnold, R. G.; Couch, H.; Little, A. M.; Smith, M. E. Involvement of cytochromes in the anaerobic biotransfor-

mation of tetrachloromethane by *Shewanella putrefaciens* 200. *Appl. Environ. Microbiol.* **1993**, *59*.
(26) Kostka, J. E.; Luther, G. W. Partitioning and speciation of solid-phase iron in saltmarsh sediments. *Geochim. Cosmochim. Acta* **1994**, *58*, 1701−1710.
(27) Stookey, L. L. Ferrozine—a new spectrophotometric reagent for iron. *Anal. Chem.* **1970**, *42*, 779−781.
(28) Roden, E. E.; Zachara, J. M. Microbial reduction of crystalline iron(III) oxides: influence of oxide surface area and potential for cell growth. *Environ. Sci. Technol.* **1996**, *30*, 1618−1628.
(29) Schwertmann, U.; Cornell, R. M. *Iron Oxides in the Laboratory*; VCH Publishers Inc.: New York, 1991.
(30) Lack, J. G.; Chaudhuri, S. K.; Kelly, S. D.; Kemner, K. M.; O'Connor, S. M.; Coates, J. D. Immobilization of radionuclides and heavy metals through anaerobic bio-oxidation of Fe(II). *Appl. Environ. Microbiol.* **2002**, *68*, 2704−2710.
(31) Villalobos, M.; Tebo, B. M. Introduction: Advances in the geomicrobiology and biogeochemistry of manganese and iron oxidation. *Geomicrobiol. J.* **2005**, *22*, 77−78.
(32) Duff, M. C.; Coughlin, J. U.; Hunter, D. B. Uranium co-precipitation with iron oxide minerals. *Geochim. Cosmochim. Acta* **2002**, *66*, 3533−3547.
(33) Ghosh, A. K.; Bhattacharyya, P. Arsenate sorption by reduced and reoxidised rice soils under the influence of organic matter amendments. *Environ. Geol.* **2004**, *45*, 1010−1016.
(34) Cooper, D. C.; Picardal, F. W.; Schimmelmann, A.; Coby, A. J. Chemical and biological interactions during nitrate and goethite reduction by *Shewanella putrefaciens* 200. *Appl. Environ. Microbiol.* **2003**, *69*, 3517−3525.
(35) Coby, A. J.; Picardal, F. W. Inhibition of NO^{3-} and NO^{2-} reduction by microbial Fe(III) reduction: Evidence of a reaction between NO^{2-} and cell surface-bound Fe^{2+}. *Appl. Environ. Microbiol.* **2005**, *71*, 5267−5274.
(36) Luu, Y. S.; Ramsay, J. A. Review: microbial mechanisms of accessing insoluble Fe(III) as an energy source. *World J. Microbiol. Biotechnol.* **2003**, *19*, 215−225.
(37) Straub, K. L.; Benz, M.; Schink, B. Iron metabolism in anoxic environments at near neutral pH. *FEMS Microbiol. Ecol.* **2001**, *34*, 181−186.

Received for review September 7, 2005. Revised manuscript received January 10, 2006. Accepted January 10, 2006.

ES051778T